

# The $\text{Al}_{50}\text{Cp}^*_{12}$ Cluster – A 138-Electron Closed Shell ( $L = 6$ ) Superatom

Peneé A. Clayborne,<sup>\*,[a]</sup> Olga Lopez-Acevedo,<sup>[a]</sup> Robert L. Whetten,<sup>[a,b]</sup> Henrik Grönbeck,<sup>[c]</sup> and Hannu Häkkinen<sup>\*,[a,d]</sup>

**Keywords:** Ab initio calculations / Aluminum / Cluster compounds / Superatoms / Shell models

Metal clusters stabilized by a surface ligand shell represent an interesting intermediate state of matter between molecular metal–ligand complexes and bulk metal. Such “metalloid” clusters are characterized by the balance between metal–metal bonds in the core and metal–ligand bonds at the exterior of the cluster. In previous studies, the electronic sta-

bility for the  $\text{Al}_{50}\text{Cp}^*_{12}$  cluster was not fully understood. We show here that the known cluster  $\text{Al}_{50}\text{Cp}^*_{12}$  can be considered as an analogue to a giant atom (“superatom”) with 138 sp electrons organized in concentric angular momentum shells up to  $L = 6$  symmetry.

## Introduction

Aluminum clusters and nanoparticles have long been studied owing to their rich chemistry and possible applications as cluster assemblies with tunable properties, as hydrogen storage materials, or as catalysts.<sup>[1]</sup> The electronic structure of bulk aluminum metal in the *fcc* lattice structure is simple, with a rather spherical Fermi surface and metallic properties of the partially filled sp conduction band derived from the atomic  $3s^23p^1$  configuration (three free electrons per atom). Very small clusters with just a few Al atoms have an incomplete sp hybridization and can exhibit multivalency and a weak tendency for directional bonding with organic ligands. The wide size range between molecule-like Al–ligand complexes and the bulk-like, metallic, larger nanoparticles includes many “metalloid” clusters, that is, systems with more Al–Al bonds than Al–ligand bonds. A series of metal-rich aluminum cluster complexes protected by Cp (cyclopentadienyl,  $\text{C}_5\text{H}_5$ ) or  $\text{Cp}^*$  (pentamethylcyclopentadienyl,  $\text{C}_5\text{Me}_5$ ) ligands has been synthesized and structurally characterized by Schnöckel and co-workers (for recent reviews, see refs.<sup>[2–4]</sup>). It is a profoundly interesting question to consider the bonding in these systems and its

effects on the physical properties as they gradually converge towards those of the bulk matter.

A remarkable metalloid cluster  $\text{Al}_{50}\text{Cp}^*_{12}$  (**1**) was reported in 2004,<sup>[5]</sup> which forms a stable intermediate step between long-known small  $\text{Al}_4\text{Cp}^*_4$  complexes and bulk Al.<sup>[6]</sup> In this communication, the underlying reasons for the stability of this cluster, arising from its special electronic structure, are analyzed and shown to be in accordance with the so-called superatom complex (SAC) model for ligand-protected metal clusters, which recently has been used successfully to describe the bonding and stability of gold clusters protected by thiolate, phosphane, and halide ligands.<sup>[7–9]</sup> This analysis provides an unambiguous view of **1** possessing 138 free sp electrons, organized in globular shells of increasing angular momentum according to Scheme 1, with  $1\text{I}^{26}$  ( $L = 6$ ) configuration for the highest occupied set of orbitals. Our analysis provides an alternative reasoning why exactly the composition 50–12 should be stable, which is complementary to the analysis recently discussed by Schnöckel and collaborators.<sup>[10]</sup> Furthermore, the electron shell view discussed here should be useful in the future to understand better the spectroscopic properties of the title cluster.



Scheme 1. Filling of angular momentum shells in a spherical system.

We used the grid-based projector-augmented wave (GPAW) DFT code<sup>[11]</sup> to optimize cluster **1** with no symmetry constraints starting from the experimental structure previously reported by Schnöckel and co-workers.<sup>[5]</sup> The technical details of the DFT calculation and the analysis of the electronic structure are given in the Experimental Section.

[a] Department of Chemistry, Nanoscience Center, University of Jyväskylä, 40014 Jyväskylä, Finland

[b] School of Chemistry and Biochemistry, Georgia Institute of Technology, Atlanta, GA 30332, USA

[c] Competence Center for Catalysis and Department of Applied Physics, Chalmers University of Technology, 41296 Göteborg, Sweden

[d] Department of Physics, Nanoscience Center, University of Jyväskylä, 40014 Jyväskylä, Finland  
Fax: +358-14-260-4756  
E-mail: Hannu.j.hakkinen@jyu.fi

Supporting information for this article is available on the WWW under <http://dx.doi.org/10.1002/ejic.201100374>.

## Results and Discussion

The  $\text{Al}_{50}\text{Cp}^*_{12}$  cluster is composed of an interior  $\text{Al}_8$  shell, surrounded by 30 aluminum atoms with an outermost shell of 12 Al atoms, which are decorated by the  $\text{Cp}^*$  ligands (Figure 1). The twelve  $\text{AlCp}^*$  units are arranged in an icosahedral symmetry. We observed that our relaxed structure agrees well with both the experimental and the previous theoretical structures (see Table 1).<sup>[5]</sup> For example, the  $\text{Al}-\text{C}_{\text{Cp}^*}$  average distance in the experimental structure is reported as 2.32 Å, while this work gives 2.33 Å (Table 1). It is interesting to note that the  $\text{Al}-\text{C}$  distance in a single  $\text{AlCp}^*$  is 2.1 Å,<sup>[12]</sup> which is slightly shorter than that found in **1**.  $\text{Al}-\text{Al}$  distances within the innermost  $\text{Al}_8$  shell, within the second  $\text{Al}_{30}$  shell, and between the outermost 12 Al atoms and the  $\text{Al}_{30}$  shell show improvement over the previous theory as well.

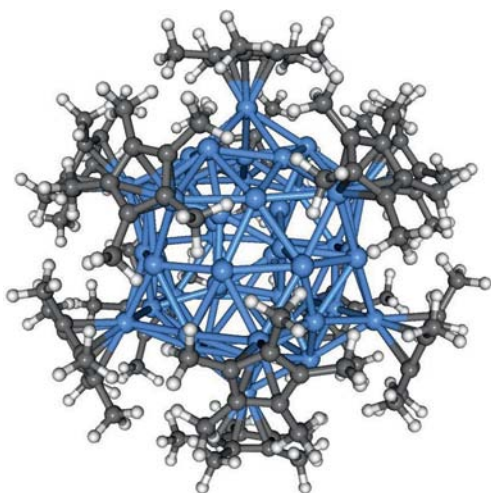


Figure 1. The optimized structure of **1**. The blue, gray, and white balls represent the aluminum, carbon, and hydrogen atoms, respectively.

Table 1. The average nearest-neighbor distances in the  $\text{Al}_{50}\text{Cp}^*_{12}$  cluster (in Å). The values calculated in this work are compared to the previously reported experimental and theoretical values.

	This work	Experiment <sup>[5]</sup>	Theory <sup>[5]</sup>
$\text{Al}-\text{Al}$	2.83	2.77	2.85
$\text{Al}-\text{C}_{\text{Cp}^*}$	2.33	2.32	2.37
$\text{C}_{\text{Cp}^*}-\text{C}_{\text{Cp}^*}$	1.42	1.42	1.44
$\text{C}_{\text{Cp}^*}-\text{C}_{\text{Me}}$	1.50	1.49	1.50
$\text{Al}_8$ shell	2.66	2.66	2.71
$\text{Al}_{30}$ shell	2.76	2.77	2.80
$\text{Al}_{30}-\text{Al}_{12}$	2.86	2.87	2.95

The (quasi)spherical geometry of the  $\text{Al}_{50}\text{Cp}^*_{12}$  cluster has previously been compared to fullerene-like structures; however, here we would like to point out the similarities to ligand-protected gold clusters. Many ligand-protected gold clusters are composed of a metallic Au core with a metallo-organic shell composed of gold–ligand units [for example, in thiolate-protected clusters, the units are  $\text{RS}(\text{AuSR})_x$  with  $x = 1$  or  $x = 2$ ].<sup>[8,13]</sup> One could view **1** in a similar fashion by assigning the  $\text{AlCp}^*$  units to the outer metallo-organic

shell [ $\text{Al}_{50}\text{Cp}^*_{12} = \text{Al}_{38}(\text{AlCp}^*)_{12}$ ].<sup>[10]</sup> Our calculated value for the binding energy of one  $\text{AlCp}^*$  unit to **1** is 1.76 eV, being somewhat larger than the previously determined tetramerization energy (around 1 eV per unit) of  $\text{Al}_4\text{Cp}^*_4$ .<sup>[14]</sup> Bader charge analysis<sup>[15]</sup> on cluster **1** reveals that each of the outer 12 aluminum atoms loses approximately 1 |e| to  $\text{Cp}^*$ , making  $\text{Cp}^*$  formally a closed-shell anion  $\text{Cp}^{*-}$ . This metal-to-ligand charge transfer is significantly higher than those in the gold/thiolate cases.

Taking into account the charge-transfer (or charge localization) effects in the metallo-organic shell, we will argue here that one can account for the number of the remaining delocalized (“itinerant”) sp electrons in cluster **1** by using the simple formula

$$n_e = N_{\text{Al}}z_{\text{Al}} - N_{\text{Cp}^*} \quad (1)$$

where  $N_{\text{Al}}$  is the total number of Al atoms,  $z_{\text{Al}} = 3$  is the valence, and  $N_{\text{Cp}^*}$  is the number of  $\text{Cp}^*$  ligands. We note that a conceptual similarity exists in relation to (i) the thiolate-protected gold clusters where Equation (1) can be used as well by considering a one-electron-withdrawing ligand, that is, the radicals  $(\text{RS}-\text{Au}-\text{SR})$  or  $(\text{RS}-\text{Au}-\text{RS}-\text{Au}-\text{SR})$  with  $z_{\text{Au}} = 1$ , and (ii) phosphane/halide-protected clusters where  $\text{AuCl}$  units take the role of  $\text{AlCp}^*$  units in **1**.<sup>[7,8]</sup>

Using Equation (1) to account for the number of sp electrons for **1**, we find  $n_e = 138$ , which is a magic number according to Scheme 1, closing the manifold of  $2\text{F}^{14}3\text{P}^61\text{I}^{26}$ . The correctness of this simple prediction can immediately be tested by analyzing the angular momentum character of the valence orbitals as described previously.<sup>[8a]</sup> The result is shown in Figure 2. It is instructive to see that **1** provides a textbook example of the orbital filling sequence,  $2\text{F}^{14}3\text{P}^61\text{I}^{26}$  indeed being the highest occupied manifold of orbitals. Owing to the (quasi)spherical  $\text{Al}_{50}$  core, the high pseudofullerene atomic symmetry results in highly degenerate orbitals in a given angular momentum shell and accordingly clear energy gaps between the shells also for the lower  $L$  values.

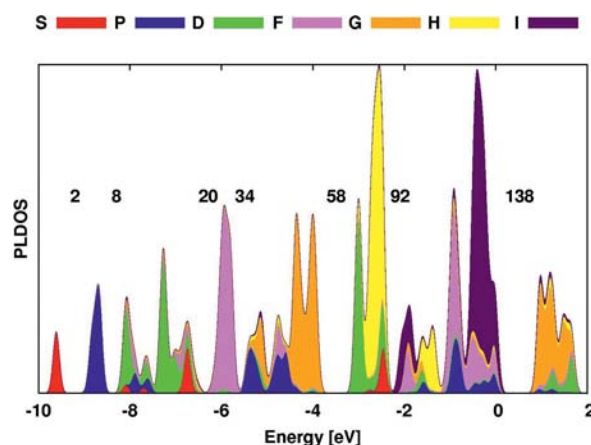


Figure 2. Projected density of states (PLDOS) for **1** with the shell closing numbers marked. The HOMO energy is set to zero.

Further manifestation of the electronic stability of **1** is shown by the appreciable HOMO–LUMO gap, calculated to be 0.9 eV, which is comparable to that of the 14-electron cluster  $\text{Au}_{38}(\text{SMe})_{24}$ ,<sup>[8]</sup> the 34-electron cluster  $\text{Au}_{39}(\text{PH}_3)_{14}\text{Cl}_6^-$  (0.8 eV),<sup>[8a]</sup> and the 58-electron cluster  $\text{Au}_{102}(\text{p-MBA})_{44}$  (0.5 eV).<sup>[8a]</sup> Our calculated values for the ionization potential and electron affinity are 4.22 eV and 1.73 eV, respectively, in line with the electronic stability of **1**. The shell-closing effects and a significant HOMO–LUMO gap reflect an increased chemical stability as well, analogously to what has been discussed in the case of “magic” gas-phase simple metal clusters.<sup>[16]</sup> A well-known case is the icosahedral  $\text{Al}_{13}^-$  anion, for which DFT calculations and recorded photoelectron spectra have shown the closing of the 40-electron shell (closing of  $2\text{P}^6$  in Scheme 1)<sup>[17]</sup> and molecular beam experiments have shown an increased stability towards oxidation.<sup>[18]</sup>

The superatomic electronic structure may explain many of the experimental observations reported for **1**. The electronic structure suggests strong metal–metal transitions based on the  $2\text{F} \rightarrow 2\text{G}$  symmetry ( $\Delta L = 1$  allowing for a strong dipole transition). Figure 3 shows that the calculated absorption spectrum of **1** has features at 2.4, 2.7, 2.9, and 3.1 eV, with a gradual increase of absorption towards blue in the visible region, in qualitative agreement with the dark red color of solutions of **1**.<sup>[5]</sup> Further implications may be found in the (dia)magnetic properties: the computed  $^{27}\text{Al}$  chemical shifts (−270 ppm, −370 ppm, +110 ppm) of **1** in solution, said to agree substantially with the solid-state NMR measurements, are quite different from those for either  $(\text{AlCp})_{1,4}$  (−90 ppm, −150 ppm) or bulk Al (+1600 ppm).<sup>[5]</sup> Using the concept of “spherical aromaticity” discussed for fullerenes and hollow metallic clusters,<sup>[19]</sup> the enormous diamagnetic shielding, experienced by both the 30-atom shell (−370 ppm) and the inner 8-atom shell (−270 ppm), may arise from “ring currents” dominantly located at the cluster surface, that is, outside the shell-of-30

but inside the shell-of-12, as required by the deshielding of the latter (+110 ppm). The surface-dominance arises because of the high  $L$  of the “frontier shell-orbitals”, particularly  $1\text{G}^{18}$ ,  $1\text{H}^{22}$ , and  $1\text{I}^{26}$ , which account for 66 of the 138 delocalized electrons.

Finally, it is interesting to note that the stability of two gallium metalloid clusters,  $\text{Ga}_{22}[\text{N}(\text{SiMe}_3)_2]_{10}^{2-}$  (**2**) and  $\text{Ga}_{23}[\text{N}(\text{SiMe}_3)_2]_{11}$  (**3**), could, in fact, be explained by using a similar electron-counting idea as applied here.<sup>[20]</sup> Both **2** and **3** can be understood as systems of 58 sp electrons, taking into account the valence  $z_{\text{Ga}} = 3$ , the one-electron-localizing nature of  $\text{N}(\text{SiMe}_3)_2$  (leaving one lone-pair at N), and the extra anionic charge of **2**. Our analysis of the angular momentum character of the frontier orbitals of **2** and **3** has confirmed this picture (to be reported later). This indicates that the power of the simple theory contained in Equation (1) extends beyond aluminum in group 13 and to the ligand  $\text{N}(\text{SiMe}_3)_2$  as well.

## Conclusions

We have shown here that the special stability of the  $\text{Al}_{50}\text{Cp}^*_{12}$  cluster can be explained within the superatom complex model in terms of the filled spherical shells of 138 delocalized Al sp electrons, in accord with Equation (1), analogously to many known ligand-protected gold clusters. On this basis, the electronic structure of **1** is consistent with the view of an aluminum core composed of fifty trivalent aluminum atoms surrounded by twelve electron-withdrawing  $\text{Cp}^*$  units. This analysis is complementary to and *not in contradiction* with the previous analysis<sup>[10]</sup> of the cluster written as  $\text{Al}_{38}(\text{AlCp}^*)_{12}$ , which also yields  $38 \times 3 + 12 \times 2 = 138$  sp electrons, since the  $\text{AlCp}^*$  may be considered as a 2-electron lone-pair donor when it is bound at the surface of the  $\text{Al}_{38}$  core (see the Supporting Information). The electron shell effects analyzed here are useful to understand optical absorption and trends found in the  $^{27}\text{Al}$  NMR diamagnetic shielding factors of **1**. This opens up the possibility to analyze, understand, and predict physical and chemical properties of analogous metalloid clusters for group 13 organometallic chemistry, giving hope that in a long run, the intermediate state of matter between “molecular” and “bulk metal” will become clear.

## Computational Details

The DFT calculations were carried out by using the grid-based projector-augmented wave (GPAW) code<sup>[11]</sup> with the generalized-gradient approximation of Perdew, Burke, and Ernzerhof (PBE) to account for the exchange–correlation interaction.<sup>[21]</sup>  $\text{H}(1\text{s})$ ,  $\text{C}(2\text{s}2\text{p})$ , and  $\text{Al}(3\text{s}3\text{p})$  electrons are treated in the valence, and the electron density is solved in a grid with 0.18 Å spacing. Cluster **1** was fully optimized with no symmetry constraints starting from the experimental structure reported in ref.<sup>[5]</sup> The structure optimization was continued until the residual forces were below 0.05 eV/Å. To analyze the superatomic electronic structure, the Kohn–Sham molecular orbitals were projected on center-of-mass spherical harmonics in a spherical volume of radius  $R_0$  including the metal core with

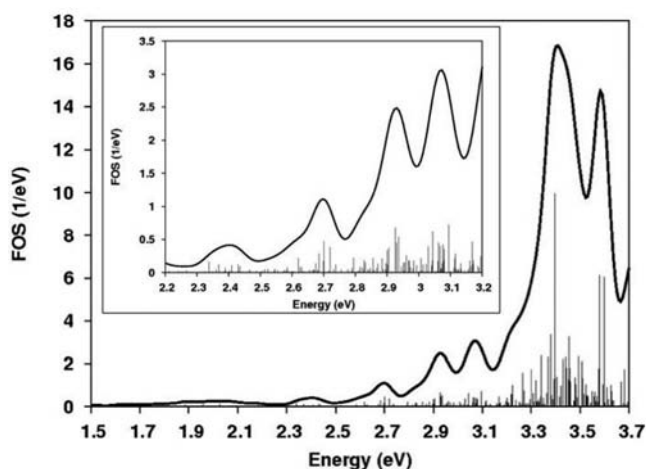


Figure 3. Theoretical photoabsorption spectrum (folded oscillator strengths, FOS) of **1**. The sticks denote the oscillator strengths of individual optical lines. The inset shows a zoomed view in the low-energy region.



the center of expansion taken to be the center of mass (ref.<sup>[8a]</sup>). The weights of different angular momenta  $L$  were calculated as

$$c_{i,L}(R_0) = \sum_M \int_0^{R_0} r^2 dr |\varphi_{i,LM}(r)|^2$$

and

$$\varphi_{i,LM}(r) = \int d\hat{r} Y_{LM}^*(\hat{r}) \psi_i(r)$$

where  $i$  is the index of the Kohn–Sham state and  $Y_{LM}$  is the spherical harmonic function. We considered angular momenta up to  $L = 6$  (I-symmetry). The optical absorption spectrum of **1** was calculated by using the linear-response time-dependent DFT (LR-TDDFT) module of the GPAW code.<sup>[11b,11c]</sup>

**Supporting Information** (see footnote on the first page of this article): Energy level diagram of the sigma donating AlCp molecule.

## Acknowledgments

H. H. acknowledges useful correspondence with A. Schnepf and H. Schnöckel. This work is supported by the Academy of Finland through projects 128341, 139614, and the Finland Distinguished Professor Program. The computer resources were provided by CSC – the Finnish IT Center for Science in Espoo.

- [1] a) P. A. Clayborne, T. C. Nelson, T. C. Devore, *Appl. Catal. A* **2004**, 257, 225; b) A. Grubisic, X. Li, S. T. Stokes, J. Cordes, J. G. F. Ganteför, K. H. Bowen, B. Kiran, P. Jena, R. Burgert, H. Schnöckel, *J. Am. Chem. Soc.* **2007**, 129, 5969; c) P. J. Roach, A. C. Reber, W. H. Woodward, S. N. Khanna, A. W. Castleman, *Proc. Natl. Acad. Sci. USA* **2007**, 104, 14565; d) P. Clayborne, N. O. Jones, A. C. Reber, J. U. Reveles, M. C. Qian, S. N. Khanna, *J. Comput. Methods Sci. Eng.* **2007**, 7, 417; e) A. W. Castleman, S. N. Khanna, *J. Phys. Chem. C* **2009**, 113, 2664; f) C. E. Bunker, M. J. Smith, K. A. S. Fernando, B. A. Harruff, W. K. Lewis, J. R. Gord, E. A. Gulians, D. K. Phelps, *ACS Appl. Mater. Interfaces* **2010**, 2, 11.
- [2] H. Schnöckel, *Dalton Trans.* **2005**, 3131.
- [3] H. Schnöckel, *Dalton Trans.* **2008**, 4344.
- [4] H. Schnöckel, *Chem. Rev.* **2010**, 110, 4125.
- [5] J. Vollet, J. R. Hartig, H. Schnöckel, *Angew. Chem.* **2004**, 116, 3248; *Angew. Chem. Int. Ed.* **2004**, 43, 3186–3189. The experimental structure has been obtained from [www.ccdc.cam.ac.uk/conts/retrieving.html](http://www.ccdc.cam.ac.uk/conts/retrieving.html). In this reference DFT was used in an implementation with local Gaussian basis functions, and the gradient-corrected Becke Perdew (BP) approximation was used for the exchange correlation functional.
- [6] M. Huber, P. Henke, H. Schnöckel, *Chem. Eur. J.* **2009**, 15, 12180.
- [7] H. Häkkinen, *Chem. Soc. Rev.* **2008**, 37, 1847.
- [8] a) M. Walter, J. Akola, O. Lopez-Acevedo, P. D. Jadzinsky, G. Calero, C. J. Ackerson, R. L. Whetten, H. Grönbeck, H. Häkkinen, *Proc. Natl. Acad. Sci. USA* **2008**, 105, 9157; b) J. Akola, M. Walter, R. L. Whetten, H. Häkkinen, H. Grönbeck, *J. Am. Chem. Soc.* **2008**, 130, 3756; c) O. Lopez-Acevedo, J. Rintala, S. Virtanen, C. Femoni, C. Tiozzo, H. Grönbeck, M. Pettersson, H. Häkkinen, *J. Am. Chem. Soc.* **2009**, 131, 12573; d) O. Lopez-Acevedo, J. Akola, R. L. Whetten, H. Grönbeck, H. Häkkinen, *J. Phys. Chem. C* **2009**, 113, 5035; e) J. Akola, K. A. Kacprzak, O. Lopez-Acevedo, M. Walter, H. Grönbeck, H. Häkkinen, *J. Phys. Chem. C* **2010**, 114, 15986; f) O. Lopez-Acevedo, H. Tsunoyama, T. Tsukuda, H. Häkkinen, C. M. Aikens, *J. Am. Chem. Soc.* **2010**, 132, 8210.
- [9] C. M. Aikens, *J. Phys. Chem. Lett.* **2011**, 2, 99.
- [10] H. Schnöckel, A. Schnepf, R. L. Whetten, C. Schenk, P. Henke, *Z. Anorg. Allg. Chem.* **2011**, 637, 15.
- [11] a) J. J. Mortensen, L. Hansen, K. W. Jacobsen, *Phys. Rev. B* **2005**, 71, 035109; b) Enkovaara, J. C. Rostgaard, J. J. Mortensen, J. Chen, M. Dulak, L. Ferrighi, J. Gavnholt, C. Glinsvad, V. Haikola, H. Hansen, H. Kristoffersen, M. Kuisma, A. Larsen, L. Lehtovaara, M. Ljungberg, O. Lopez-Acevedo, P. Moses, J. Ojanen, T. Olsen, V. Petzold, N. Romero, J. Stausholm-Moller, M. Strange, G. Tritsarlis, M. Vanin, M. Walter, B. Hammer, H. Häkkinen, G. Madsen, R. Nieminen, J. Norskov, M. Puska, T. Rintala, J. Schiotz, K. Thygesen, K. W. Jacobsen, *J. Phys. Condens. Matter* **2010**, 22, 253202; c) Walter, M. H. Häkkinen, L. Lehtovaara, J. M. Puska, J. Enkovaara, C. Rostgaard, J. J. Mortensen, *J. Chem. Phys.* **2008**, 128, 244101; The GPAW code is freely available at <https://wiki.fysik.dtu>.
- [12] P. Jutzi, N. Burford, *Chem. Rev.* **1999**, 99, 969.
- [13] H. Häkkinen, M. Walter, H. Grönbeck, *J. Phys. Chem. B* **2006**, 110, 9927.
- [14] a) R. Ahlrichs, M. Ehrig, H. Horn, *Chem. Phys. Lett.* **1991**, 183, 227; b) M. Huber, H. Schnöckel, *Inorg. Chim. Acta* **2008**, 361, 457.
- [15] a) R. F. W. Bader, *Atoms in Molecules*, Clarendon Press, Oxford, **1990**; b) W. Tang, E. Sanville, G. J. Henkelman, *J. Phys. Condens. Matter* **2009**, 21, 7.
- [16] W. A. de Heer, *Rev. Mod. Phys.* **1993**, 65, 611.
- [17] a) S. N. Khanna, P. Jena, *Phys. Rev. Lett.* **1992**, 69, 1664; b) S. N. Khanna, P. Jena, *Phys. Rev. B* **1995**, 51, 13705; c) J. Akola, M. Manninen, H. Häkkinen, U. Landman, X. Li, L. S. Wang, *Phys. Rev. B* **1999**, 60, R11297.
- [18] a) R. E. Leuchtner, A. C. Harms, A. W. Castleman, *J. Chem. Phys.* **1989**, 91, 2753; b) D. E. Bergeron, A. W. Castleman Jr., T. Morisato, S. N. Khanna, *Science* **2004**, 304, 84.
- [19] a) M. P. Johansson, D. Sundholm, J. Vaara, *Angew. Chem.* **2004**, 116, 2732; *Angew. Chem. Int. Ed.* **2004**, 43, 2678; b) M. P. Johansson, J. Vaara, D. Sundholm, *J. Phys. Chem. C* **2008**, 112, 19311; c) A. J. Karttunen, M. Linnolahti, T. A. Pakkanen, P. Pyykkö, *Chem. Commun.* **2008**, 465.
- [20] a) A. Schnepf, G. Stösser, H. Schnöckel, *Angew. Chem.* **2002**, 114, 1959; *Angew. Chem. Int. Ed.* **2002**, 41, 1882; b) J. Hartig, A. Stösser, P. Hauser, H. Schnöckel, *Angew. Chem.* **2007**, 119, 1687; *Angew. Chem. Int. Ed.* **2007**, 46, 1658–1662.
- [21] J. P. Perdew, K. Burke, M. Ernzerhof, *Phys. Rev. Lett.* **1996**, 77, 3865.

Received: April 7, 2011

Published Online: May 13, 2011